

# Nanoscale

Accepted Manuscript



This is an *Accepted Manuscript*, which has been through the RSC Publishing peer review process and has been accepted for publication.

*Accepted Manuscripts* are published online shortly after acceptance, which is prior to technical editing, formatting and proof reading. This free service from RSC Publishing allows authors to make their results available to the community, in citable form, before publication of the edited article. This *Accepted Manuscript* will be replaced by the edited and formatted *Advance Article* as soon as this is available.

To cite this manuscript please use its permanent Digital Object Identifier (DOI®), which is identical for all formats of publication.

More information about *Accepted Manuscripts* can be found in the [Information for Authors](#).

Please note that technical editing may introduce minor changes to the text and/or graphics contained in the manuscript submitted by the author(s) which may alter content, and that the standard [Terms & Conditions](#) and the [ethical guidelines](#) that apply to the journal are still applicable. In no event shall the RSC be held responsible for any errors or omissions in these *Accepted Manuscript* manuscripts or any consequences arising from the use of any information contained in them.

Cite this: DOI: 10.1039/c0xx00000x

www.rsc.org/xxxxxx

**PAPER**

## Light-responsive polymer nanoreactor: A source of reactive oxygen species on demand

Patric Baumann,<sup>a</sup> Vimalkumar Balasubramanian,<sup>a</sup> Ozana Onaca-Fischer,<sup>a</sup> Andrzej Sienkiewicz<sup>b</sup> and Cornelia G. Palivan<sup>\*,a</sup>

<sup>5</sup> Received (in XXX, XXX) Xth XXXXXXXXX 20XX, Accepted Xth XXXXXXXXX 20XX

DOI: 10.1039/b000000x

Various domains present the challenges of responding to stimuli in a specific manner, with the desired sensitivity or functionality, and only when required. Stimuli-responsive systems that are appropriately designed can effectively meet these challenges. Here, we introduce nanoreactors that encapsulate photosensitizer-protein conjugates in polymer vesicles as a source of “on demand” reactive oxygen species. Vesicles made of poly-(2-methyloxazoline)-poly (dimethylsiloxane)-poly (2-methyloxazoline) successfully encapsulated the photosensitizer Rose Bengal-bovine serum albumin conjugate (RB-BSA) during a self-assembly process, as demonstrated by UV-Vis spectroscopy. A combination of light scattering and transmission electron microscopy indicated that the nanoreactors are stable over time. They serve a dual role: protecting the photosensitizer in the inner cavity, and producing *in situ* reactive oxygen species (ROS) upon irradiation with appropriate electromagnetic radiation. Illumination with appropriate wavelength light allows us to switch on/off and to control the production of ROS. Because of the oxygen-permeable nature of the polymer membrane of vesicles, ROS escape into the environment around vesicles, as established by electron paramagnetic resonance. The light-sensitive nanoreactor is taken up by HeLa cells in Trojan horse fashion: it is nontoxic and, when irradiated with the appropriate laser light, produces ROS that induce cell death in a precise area corresponding to the irradiation zone. These nanoreactors can be used in theranostic approaches because they can be detected via the fluorescent photosensitizer signal and simultaneously produce ROS efficiently “on demand”.

### Introduction

Design of stimuli-responsive systems, where a rapid and specific response to changes in environmental conditions serves to sense-/deliver molecules or to induce processes, is in focus today in various domains such as medicine, material science, food science. Stimuli-responsive systems containing polymers are based either on a responsive polymer or on a combination of a responsive compound and a polymer supramolecular assembly serving as the carrier/template for the compound. A smart response to external or internal stimuli facilitates controlled release of a payload at a desired region, precise activity modulated by stimuli, or rapid imaging of a pathological event.<sup>1</sup> A large variety of polymers have been synthesized to respond to physical, chemical or biological stimuli by undergoing dramatic physical or chemical changes in reply to stimulus presence.<sup>2</sup> One important feature of this type of material is reversibility, i.e. the ability of the polymer to return to its initial state upon application of a stimulus for a defined period of time.

In particular, polymer supramolecular assemblies such as micelles, capsules, and vesicles reply to a stimulus by changing their architecture or properties.<sup>3</sup> Polymers have proven themselves clever options in developing stimuli-responsive

systems because their chemical nature permits modulating their properties by including responsiveness via sensitive chemical moieties. Typically, the ‘response’ of a polymer in solution is based on changes to its individual chain size, secondary structure, solubility, or degree of intermolecular association.<sup>4</sup> Systems that are based on a dramatic alteration of the polymer structure inducing a disintegration of their architecture during their contact with the stimulus, and subsequent release of payload, represent the majority of the stimuli-responsive materials reported so far.<sup>5</sup> Meanwhile, there is a limited number of polymer supramolecular assemblies that contain responsive payloads and that preserve assembly architecture while the active compound acts inside when in contact with the stimulus. Polymer vesicles containing a pH-controlled enzyme have been described as a first example of a biohybrid nanoreactor that responds to pH changes present outside the polymer assemblies.<sup>6</sup> The pH-responsive system is described as a model that can be further exploited for medical applications.

Nanoreactors consist of compartments, for example polymer vesicles, that encapsulate an active molecule/combination of molecules protected from degradation inside the compartment, and simultaneously acting *in situ*.<sup>7</sup> Various types of nanoreactors have been introduced by the encapsulation of enzymes or mimics.<sup>8-10</sup> However, to act in a stimuli-responsive manner, with

a rapid, easy switching on/off, nanoreactors have to be designed with stimuli-responsive active compounds and should avoid limitations that could result from the consumption of reactants, or activity in other regions/times than those desired.

Here, we introduce stimulus-responsive nanoreactors based on the encapsulation of a highly active photosensitizer-protein conjugate in polymer nanovesicles. Stimulus-responsiveness is obtained by the property of the photosensitizer-protein conjugate, generating *in situ* ROS in the cavities of the nanoreactors only when irradiated with the corresponding wavelength of light (Figure 1). ROS production can thus be switched on/off and controlled by appropriate light-irradiation. We selected poly(2-methyloxazoline)-block-poly(dimethylsiloxane)-block-poly(2-methyloxazoline) (PMOXA-PDMS-PMOXA) triblock copolymer, which has already been reported to generate stable, self-assembled vesicular structures in aqueous media<sup>8</sup> with oxygen permeable membranes.<sup>11</sup> Due to the specific chemistry of the PMOXA-PDMS-PMOXA, which renders the membrane permeable to ROS but impermeable to small molecules such as water or urea,<sup>12</sup> nanoreactors will preserve the photosensitizer-protein conjugate inside, while allowing *in situ* generated ROS to escape the vesicle. In addition, both polymer vesicles and nanoreactors based on PMOXA-PDMS-PMOXA copolymers have already been shown to be taken-up and to preserve their morphology inside cells.<sup>13</sup> Improvement of up-take has been reported by functionalisation with specific molecules (antibodies or ligands), which leads to the successful targeting of desired cells.<sup>14, 15</sup>

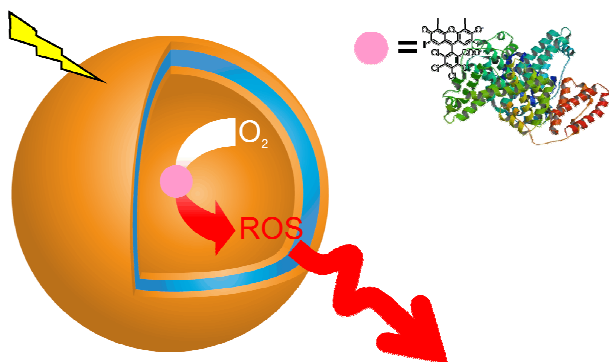


**Fig. 1** Schematic representation of polymeric nanoreactors that serve as a source of reactive oxygen species “on demand”. When irradiated with an appropriate wavelength, and in the presence of oxygen, the photosensitizer-protein conjugate generates ROS, which pass through the polymer membrane in the environment of vesicles.

We chose a photoactive dye, Rose Bengal (RB), as the active molecule in the nanoreactor,<sup>16</sup> because this di-anionic photosensitizer is known to convert oxygen to reactive oxygen species (ROS), such as  $O_2^{\cdot-}$  and  $^1O_2$  with a high quantum yield.<sup>17, 18</sup> Photosensitizers have already been used to produce ROS for the treatment of age-related macular degeneration, burns, ulcers, cancer and dermal applications.<sup>19, 20</sup> To increase RB hydrophilicity, and therefore to improve the encapsulation efficiency, RB was conjugated to the stable and robust protein, bovine serum albumin (BSA).<sup>21</sup> We investigated, by a combination of spectroscopy and electron spin resonance (ESR), *in situ* production of ROS, while light scattering (LS) and

transmission electron microscopy (TEM) allowed us to assess the morphology and stability of nanoreactors before and after light-irradiation.

Our system will act like a Trojan horse to induce cell death “on demand,” because it is designed to be taken-up by cells with no consequent toxicity, while inducing cell death upon production of ROS under laser light irradiation at a specific wavelength. Our nanoreactors support theranostic approaches because they play a dual role: the role needed in diagnostic application – easy detection – and that required in therapeutics – inducing cell death under controlled circumstances<sup>22</sup>. As an example of possible medical application, we tested our light-responsive nanoreactors in cell lines for photodynamic therapy (PDT), which is expected to gain full potential if drawbacks such as the inherent systemic toxicity of photosensitizers<sup>23, 24</sup> can be eliminated by nanoreactor use.

## Experimental

Chemicals were purchased from *Sigma-Aldrich* at the highest purity and were used without further treatment.

### Polymer synthesis

We used the copolymer PMOXA<sub>10</sub>-PDMS<sub>87</sub>-PMOXA<sub>10</sub>, as synthesized by Egli *et al.* (Figure S1).<sup>25</sup>

**Rose Bengal – BSA conjugation:** 20 mg (300  $\mu$ M) bovine serum albumin (BSA) were dissolved in 1 ml PBS solution containing 100  $\mu$ M Rose Bengal (RB). After 1 h at room temperature the solution was applied to a HiTrapDesalting column containing Sephadex<sup>TM</sup> Superfine (GE Healthcare, UK).

### RB-BSA encapsulation in polymer vesicles

The film rehydration method was used to prepare vesicles with encapsulated RB-BSA conjugates.<sup>26</sup> 5 mg of PMOXA<sub>10</sub>-PDMS<sub>87</sub>-PMOXA<sub>10</sub> were dissolved in EtOH and transferred into a 10 ml round-bottom flask. EtOH was evaporated at a reduced pressure of 150 mbar in a rotary vacuum evaporator (Büchi Rotavapor R-124 with vacuum controller B-721, Büchi Switzerland) at 40 °C, while rotating at 100 rpm to obtain a polymer film on the inner glass surface of the flask. 1 ml PBS containing RB-BSA conjugates (50  $\mu$ M RB; 150  $\mu$ M BSA) was added to the film under continuous stirring overnight at room temperature under atmospheric pressure. The obtained vesicle solution was extruded with a LiposoFast-Basic extruder (Avestin, Canada) through a 0.2  $\mu$ m Nucleopore Track-Etch membrane from *Whatman* (11 times). The extruded vesicle solution was applied to a size exclusion chromatography (SEC) column filled with Sepharose 2B connected to an ÄKTA prime (GE Healthcare, UK). Control vesicles were prepared by applying a solution to the Sepharose 2B column, containing a premix of 500  $\mu$ l 5 mg/ml empty polymer vesicles and 500  $\mu$ l RB-BSA conjugate solution. The control vesicles were tested after SEC for the presence of RB and BSA by UV-Vis spectroscopy at 560 nm and SDS-PAGE, respectively.

### Rose Bengal – BSA conjugate detection

A calibration curve based on the absorbance maxima at 560 nm of a RB-BSA conjugate was established, with a dilution series ranging from 1  $\mu$ M to 100  $\mu$ M RB-BSA conjugate

concentrations. The SEC-fraction-containing vesicles with encapsulated RB-BSA conjugates were analysed with UV-Vis spectroscopy (SpectraMax M5<sup>e</sup>, Molecular Devices, USA) at 560 nm. The absorbance curves were background corrected and the obtained intensities were compared with the standards resulting from the dilution series. The volumes of the fraction containing RB-BSA nanoreactors were determined in order to calculate the volume-corrected encapsulation efficiency.

### Light scattering

Light scattering experiments were performed using an ALV goniometer (ALV GmbH, Germany) equipped with an ALV He-Ne laser (JDS Uniphase, wavelength  $\lambda = 632.8$  nm). The vesicle solution (1 mg/ml, 0.5 mg/ml, 0.4 mg/ml and 0.33 mg/ml) was measured in a 10 mm cylindrical quartz cell at angles ranging from 40° to 150° at 273 K. ALV / Static & Dynamic FIT and PLOT program version 4.31 10/10 was used in the process. Static light scattering data were processed according to the Guinier-model.

### Transmission electron microscopy

10  $\mu$ l empty polymer vesicle solution and an RB-BSA conjugate-loaded polymer vesicle solution were negatively stained with 2% uranyl acetate solution and deposited on a carbon-coated copper grid. The samples were examined with a transmission electron microscope (Philips Morgani 268 D) operated at 80 kV.

### Electron spin resonance

TMP-OH powder was weighed and a solution with the same amount of RB was added to the powder to obtain a concentration of 200  $\mu$ M. In the case where RB, RB-BSA, and the vesicle solution did not have the same absorbance at 550 nm and 560 nm, the sample was diluted with PBS until they all had the same RB concentration. The ESR experiments were carried out at room temperature using an ESP300E spectrometer (Bruker BioSpin, Germany) operating at the X-band frequency and equipped with a standard rectangular mode TE<sub>102</sub> cavity. Samples were transferred to 0.7 mm ID and 0.87 mm OD glass capillary tubes (VetroCom, NJ, USA), with sample height  $\sim$  50 mm ( $\sim$ 20 microliter), and sealed on both sides with Cha.seal (tube sealing compound, Chase Scientific Glass, Rockwood, TN, USA). An assembly of seven tightly packed capillaries was bundled together and inserted into a wide-bore quartz capillary (standard ESR quartz tube with 2.9 mm ID and 4 mm OD, Model 707-SQ-250M, from WilmadGlass Inc., Vineland, NJ, USA) This setup resulted in ca. 140 microliter sample volume in the active zone of the TE<sub>102</sub> cavity. The samples were illuminated with visible light and measured with the typical instrument setting: microwave frequency 9.77 GHz, microwave power 10.1 mW, sweep width 100 G, modulation frequency 100 kHz, modulation amplitude 0.5 G, receiver gain  $2 \times 10^4$ , time constant 81.92 ms, conversion time 40.96 ms and total scan time 41.9 s.

### Cell toxicity assay

$2 \times 10^4$  HeLa cells per well were cultured in Dulbecco's Modified Eagle's Medium (DMEM) containing 10% fetal calf serum (FCS) for 24 h in a 96-well plate and then incubated with different concentrations of polymersomes [50, 100, 200, 300  $\mu$ g/ml]. The cells were grown for another 24 h in the presence of the

polymersomes at 37 °C and 5% CO<sub>2</sub> atmosphere. Cell viability was tested using the MTS (3-(4,5-dimethylthiazol-2-yl)-5-(3-carboxymethoxyphenyl)-2-(4-sulfophenyl)-2H-tetrazolium) assay (Promega, USA). After 1 h of incubation with MTS the absorbance of each well was measured at 490 nm with a microplate reader (SpectraMax M5, Molecular Devices, USA)

### Uptake studies and photosensitizing activity tests

HeLa cells were cultured at a density of  $5 \times 10^4$  cells per well in an 8-well Lab-Tek<sup>TM</sup> (Nalge Nunc International, USA) for 24 h in DEME growth medium to allow attachment to the surface. After attachment, the medium was removed and polymer vesicles containing RB-BSA conjugates were added and incubated for an additional 20 h in DEME growth medium without FCS. The pre-treated HeLa cells containing the RB-BSA nanoreactors were further incubated at 37 °C with freshly prepared Deep Red (Cellmask<sup>TM</sup>) plasma membrane stain (5  $\mu$ g/ml) and Hoechst 3342 (5  $\mu$ g/ml) dsDNA stain for 10 min. The cells were washed three times with PBS buffer and visualized with a confocal laser scanning microscope (Carl Zeiss LSM510, Germany) equipped with a 63x water emulsion lens (Olympus, Japan). The measurements were performed in multitrack mode, and the intensity of each fluorescent dye was adjusted individually: Hoechst 3342 was excited at 405 nm in channel 1, Deep Red at 633 nm in channel 2 and RB-BSA at 543 nm in channel 3. The images were recorded using Carl Zeiss LSM software (version 4.2 SP1).

During irradiation experiments, cells were visualized first using 405 nm and 633 nm lasers. The 543 nm laser was used as an excitation source for the cells in a defined area at 23.7 J/cm<sup>2</sup>. Subsequently, the area was visualized using 405 nm and 633 nm laser light. This was repeated several times followed by a visualization of a larger area that included the defined area.

## Results and discussion

We generated the stimulus-responsive nanoreactors in a straightforward manner: the self-assembly process of amphiphilic copolymers in the presence of photosensitizers induced the formation of supramolecular assemblies containing the photosensitizers inside. The inherent conditions that support the functionality of a nanoreactor are high encapsulation efficiency for the active compound (in our case the photosensitizer), and the ability of that photosensitizer to act *in situ*, inside the polymer assembly. In this respect we first improved the solubility of the photosensitizer that we chose as the active compound.

### Nanoreactors: generation and characterisation

In order to improve solubility and therefore increase the encapsulation efficiency, we conjugated the photosensitizer RB with bovine serum albumin (BSA), which is known to be stable and favors a hydrophobic interaction with RB.<sup>27, 28</sup> In addition, the conjugation of RB to BSA avoids interaction with the polymer membrane due to the hydrophilic character of BSA. The successful conjugation was proved by the shift in the maximum absorbance from  $\lambda = 547$  nm to  $\lambda = 559$  nm (Figure S2).<sup>[35]</sup> To encapsulate RB-BSA photosensitizers inside polymer assemblies of PMOXA<sub>10</sub>-PDMS<sub>87</sub>-PMOXA<sub>10</sub> we used the film rehydration

method.<sup>26</sup>

The nanoreactors were extruded to control their size and reduce polydispersity and further purified by size exclusion chromatography (SEC). To determine whether RB-BSA conjugates bind unspecifically to the nanoreactors, all fractions obtained after purification of a mixture of empty polymer assemblies and RB-BSA were collected and loaded onto SDS acrylamide gel; no RB-BSA conjugate was present in the vesicle

fraction (Figure S3). This shows that RB-BSA does not interact with the polymer membrane, as expected, due to the hydrophilic character of BSA. In addition fluorescence measurements indicate that there is no change in the emission wavelength of RB-BSA both in the presence of polymer vesicles, and when it is encapsulated in nanoreactors (Figure S4). Therefore, during the self-assembly process of vesicles formation, RB-BSA is encapsulated in the aqueous cavity of vesicles.

**Table 1** Static and dynamic light scattering data for polymer vesicles and RB-BSA nanoreactors. The radius of gyration ( $R_g$ ) and the hydrodynamic radius ( $R_h$ ) were calculated with SLV/static & Dynamic Fit and PLOT software (Figure S5).

	$R_g$	$R_h$	$M_w, \text{g mol}^{-1}$	$A_2 \text{ mol dm}^3/\text{g}^2$	$R_g/R_h$
Empty vesicles	$107 \pm 3 \text{ nm}$	$112 \pm 3 \text{ nm}$	$1.83 \times 10^9$	$3.388 \times 10^{-10}$	0.96
RB-BSA nanoreactors	$105 \pm 2 \text{ nm}$	$110 \pm 2 \text{ nm}$	$1.33 \times 10^9$	$2.662 \times 10^{-10}$	0.95
After one month at room temperature					
Empty vesicles	$106 \pm 2 \text{ nm}$	$115 \pm 3 \text{ nm}$	$1.18 \times 10^9$	$3.388 \times 10^{-10}$	0.96
RB-BSA nanoreactors	$103 \pm 4 \text{ nm}$	$109 \pm 5 \text{ nm}$	$1.34 \times 10^9$	$2.712 \times 10^{-10}$	0.95

Nanoreactors were characterized using light scattering and transmission electron microscopy, and compared with polymer assemblies without photosensitizers (Table 1). In both cases the ratios of  $R_g$  to  $R_h$  were calculated to values close to 1, showing that nanoreactors and polymer assemblies are made of vesicles.<sup>29</sup>

Similar sizes in both cases indicate that the encapsulation of photosensitizers affect neither the morphology of polymer assemblies, nor their size. Our analysis yields  $A_2$  values  $\approx 0$ , within experimental error (*i.e.*, no long-range interactions between the vesicles in the concentration range investigated).

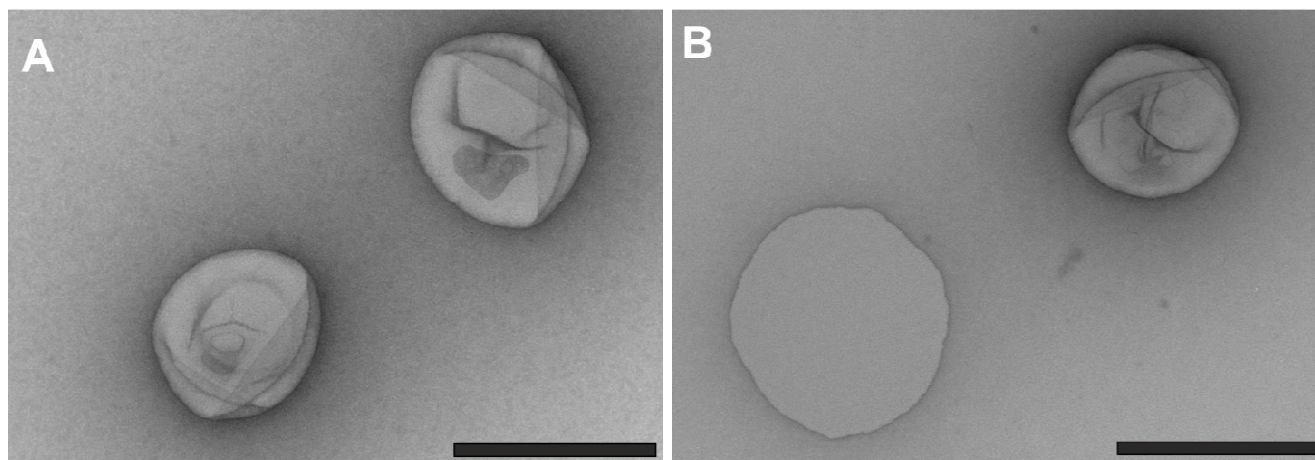
Transmission electron microscopy (TEM) micrographs of empty vesicles (Figure 2A) and RB-BSA nanoreactors (Figure 2B) reveal collapsed vesicular structures in good agreement with the light scattering data. The stability of nanoreactors over time is an important parameter for their application; to determine stability, nanoreactors were stored for one month at room temperature while protected from light. The obtained values of  $R_g$  and  $R_h$  did

not change over this period (Table 1), an observation supported by TEM micrographs as well. Stability studies with PMOXA-PDMS-PMOXA vesicles with different block lengths in blood plasma showed stability over several hours.<sup>30</sup> Illumination of vesicles/nanoreactors with light (405 nm, 543 nm, and 633 nm) did not change the morphology or size of vesicles. The high stability of polymer vesicles supports their prospective applications in medicine and technology.

The concentration of RB-BSA conjugates inside the cavity of nanoreactors was estimated by comparing them spectroscopically with a dilution series of known RB-BSA concentrations. The volume-corrected encapsulation efficiency was calculated as 13% (4  $\mu\text{M}$  concentration of RB-BSA inside nanoreactors). The quantity of RB-BSA conjugates inside the nanoreactors was at the same order of magnitude as that previously used for other PDT studies (10 – 40  $\mu\text{M}$  RB).<sup>31</sup>

Cite this: DOI: 10.1039/c0xx00000x

www.rsc.org/xxxxxx

**PAPER**

**Fig. 2** TEM micrographs of freshly prepared: polymer vesicles A), and RB-BSA nanoreactors B) (black scale bars: 200 nm).

### Nanoreactor activity

While the conjugation of RB to peptides was shown not to inhibit the photoactive property,<sup>32</sup> the effect of conjugation with the BSA protein has not been reported. Therefore, we first investigated the photodynamic activities of RB and RB-BSA conjugates using ESR. The formation of  $^1\text{O}_2$  upon illumination of RB/RB-BSA conjugates with a visible light source was followed by means of the appearance of a paramagnetic species as the product of the reaction of  $^1\text{O}_2$  and a scavenging molecule. We selected 2,2,6,6-tetramethyl-4-piperidinol, TMP-OH, as the scavenging molecule because it is diamagnetic and therefore ESR silent (**Figure 3**). Upon reaction with  $^1\text{O}_2$ , it produces TEMPOL, a paramagnetic species, with a well resolved ESR spectrum, the integral of which is proportional to the amount of  $^1\text{O}_2$ .<sup>33</sup> In addition, the formation of TEMPONE, a product of the partial decay of TEMPOL due to attack by  $\text{O}^{2-}$ , can be observed by ESR as well.

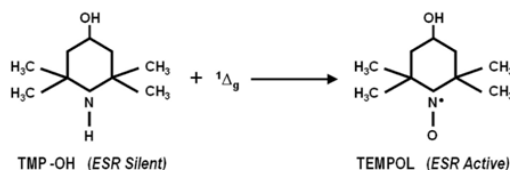


**Fig. 3** TMP-OH, as an ESR silent molecule, reacts in the presence of  $^1\Delta_g$  to form TEMPOL, which is detectable via ESR measurement.

The RB/RB-BSA conjugate solutions were first measured with ESR without illumination: no ESR signal was obtained. Upon homogeneous illumination with visible light for increasing periods of time (up to 20 minutes), ESR spectra indicated the formation of paramagnetic species. We observed not only the formation of TEMPOL ( $g = 2.0055$ ,  $a_N = 17.13$  G) but also the formation of TEMPONE ( $g = 2.0054$ ,  $a_N = 16.13$  G) (**Figure 4A**).

The integrals of the ESR spectra were used as a quantitative value for TEMPOL and TEMPONE concentration. As expected, RB was able to produce TEMPOL and TEMPONE at the highest efficiency (**Figure 4B-a**). RB-BSA conjugates preserved 70% of photodynamic activity after 20 min illumination (**Figure 4B-b**). Due to the high photodynamic efficiency of RB, the ROS generated by RB-BSA conjugates is high enough for application in medical domain, for example to PDT. In addition, the photodynamic activity of the conjugate can be further improved by using an appropriate laser light source that is known to have a higher efficiency in activating RB.<sup>27</sup> ESR was further used to study the generation of ROS inside nanoreactors, and their escape through the polymer membrane. It was already proven that the PMOXA-PDMS-PMOXA membrane is permeable to ROS,<sup>11</sup> while it is not permeable to small molecules, such as water.<sup>12, 13, 34</sup> As the nanoreactor membrane is impermeable to TMP-OH, its conversion to the stable TEMPOL and TEMPONE paramagnetic species takes place only outside the vesicles. Therefore, the formation of TEMPOL and TEMPONE in the environment of vesicles represents a direct indicator of the production of ROS inside the nanoreactor, and their escape through the polymer membrane. For comparable results of ESR measurements, solutions containing RB, RB-BSA conjugates and RB-BSA nanoreactors were diluted to the same RB concentration, which was determined with UV-VIS spectroscopy by making a comparison at absorbance intensity of  $\lambda = 550$  nm and  $\lambda = 560$  nm. ESR spectra of RB, RB-BSA and RB-BSA nanoreactors were measured with and without increasing illumination times under similar conditions as mentioned above. Spectra integrals indicate that, after 20 min illumination, RB-BSA conjugates and RB-BSA nanoreactors preserved around 70% of the initial photodynamic activity of RB (**Figure 4B-b** and **c**). As there is no significant difference in the photodynamic efficiency when RB-BSA is encapsulated in the polymer vesicles, this clearly indicates that the polymer membrane does not

influence the efficacy of the nanoreactors in terms of the ROS amount provided outside the vesicles. As expected, empty

polymer vesicles were not been involved in the production of ROS upon irradiation (they were ESR silent, Figure 4B-d).

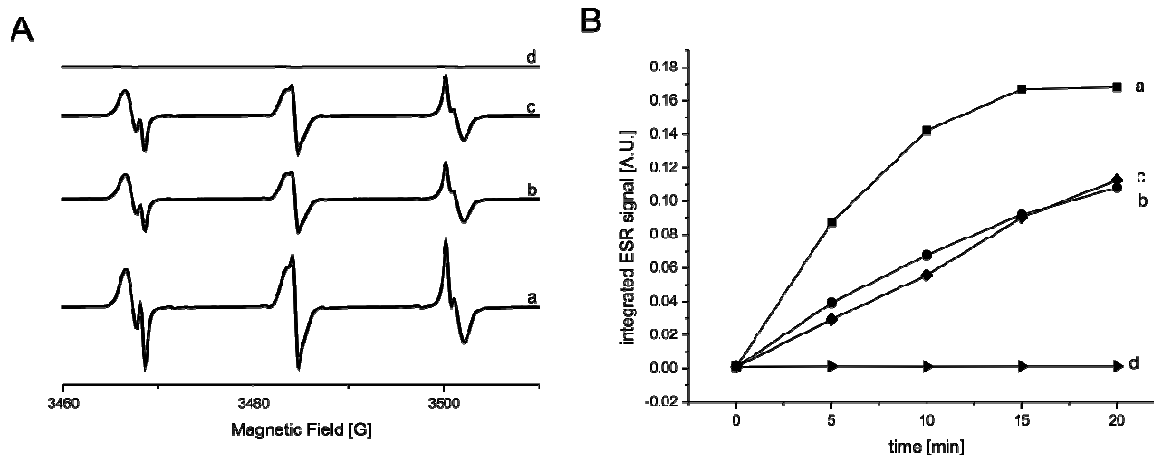
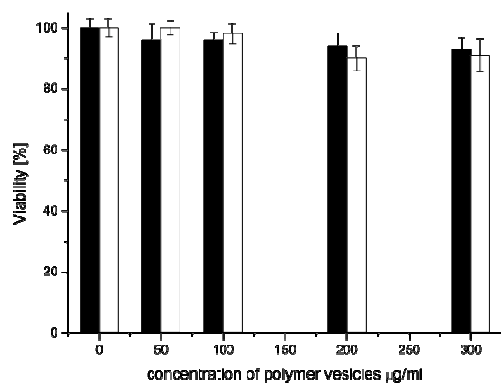


**Fig. 4** A) ESR spectra of: RB (a), RB-BSA conjugates (b), nanoreactors (c) and empty vesicles (d). B) Integrals of the ESR spectra as a function of illumination time for: RB (a, ■), RB-BSA (b, ●), nanoreactors (c, ◆), and empty vesicles (d, ►).

### ROS production “on demand” by nanoreactors inside cells

The internalization, stability, and *in situ* activity of nanoreactors have been tested on HeLa cancer cells. For further medical applications it is important that RB-BSA nanoreactors be delivered to cells without being denatured and with low dark toxicity (damage to cells in dark conditions). There was no noticeable difference in cell viability between cells incubated with polymer vesicles/nanoreactors, and untreated HeLa cells, as measured using an MTS assay. Cell viability was over 90% up to a polymer vesicle concentration of 300  $\mu\text{g/ml}$  (Figure 5). In addition, there was no difference in dark toxicity between empty vesicles and nanoreactors (polymer vesicle concentration between 50 and 300  $\mu\text{g/ml}$ ), in agreement with previous reports on low cytotoxicity of PMOXA-PDMS-PMOXA polymer vesicles with



different block lengths, in other cell lines.<sup>35, 36</sup>

**Fig. 5** HeLa cell viability after 24 h incubation in dark conditions with: nanoreactors (black), and empty vesicles (white). Untreated cells are considered 100% viable.

We used laser scanning microscopy (LSM) to examine both the uptake and the photosensitizing activity of RB-BSA-containing

nanoreactors in HeLa cells. In normal culture conditions, untreated HeLa cells form a semi-confluent layer composed of individual, adhered, flat cells, both in dark and when illuminated by light (Figure 5A). To improve the uptake of nanoreactors, HeLa cells were incubated with polymer vesicles/nanoreactors in a medium without bovine calf serum, to favour uptake. In the intracellular regions of damaged cells (Figure 6B) we observed a fluorescent signal specific for the RB-BSA-conjugate, which has the excitation wavelength at 543 nm (Figure S4). As PMOXA-PDMS-PMOXA vesicles are stable inside cells for more than 48 hours,<sup>13, 35</sup> and RB-BSA cannot escape from their cavities; the fluorescent signal in LSM micrographs clearly indicates the uptake of nanoreactors (Figure 6B and 6C).

To test the stimulus-responsive activity of RB-BSA nanoreactors, HeLa cells incubated with nanoreactors were irradiated with various laser wavelengths (405, 543, and 633 nm). Upon irradiation with 543 nm laser light the nanoreactors become fluorescent (red dots), and therefore their up-take can be observed. After irradiation with 543 nm laser wavelength the cell membranes of HeLa cells that have nanoreactors taken-up start to shrink and form blebs after a few tens of seconds of irradiation, while normal cells untreated with nanoreactors preserve their shape and integrity. Formation of blebs has already been reported for HeLa cells when RB was irradiated *in situ* by a laser with a wavelength of 530 nm, but only 24 h after irradiation.<sup>37</sup> Here, we observed significant bleb formation within a few minutes after the irradiation of nanoreactor-containing cells, at a laser intensity of 23.7  $\text{J/cm}^2$ . The irradiation conditions that we chose are similar to normal PDT treatment conditions (dose 30 – 135  $\text{J/cm}^2$  and time 5 – 30 min), in order to investigate possible application in the medical domain.<sup>38-40</sup> Controlled production of ROS was obtained by varying the illumination time and the laser intensity. The significant decrease in the time necessary to induce cell death when nanoreactors are active allows a decrease in the overall dose of irradiation necessary to produce a required cytotoxic effect. The longer the time of irradiation, the larger the blebs and the greater the cell deaths induced. The formation of blebs was

only observed for cells exposed to a laser wavelength of 543 nm (Figure 6E), but not to other wavelengths of 405 nm and 633 nm (Figure 5D). In cells incubated for 24 hours with RB-BSA nanoreactors and irradiated with an inappropriate wavelength, no visible phototoxic effect was observed, with cells preserving the integrity of their plasma membrane and remaining intact (Figure 6D).<sup>[44]</sup>

Moreover, cells incubated for 24 hours with nanoreactors that were close to the area irradiated with 543 nm laser (white square area in Figure 6F), but not directly exposed to irradiation, preserved their integrity (environment of white square area,

Figure 6F). Together with the significant changes in cell integrity when irradiated with the appropriate laser wavelength, this indicates that the nanoreactors generate ROS only “on demand” and that the affected area corresponds to the irradiation surface. In this respect, the stimulus-responsive RB-BSA nanoreactors serve to produce ROS in the desired region, but without affecting other close regions. Irradiation for longer periods of time (up to 10 minutes) induced severe changes in cell morphology up to the death of cells. This clearly indicates the mediated ROS phototoxicity of RB-BSA nanoreactors when switched on by irradiation of the appropriate laser wavelength.

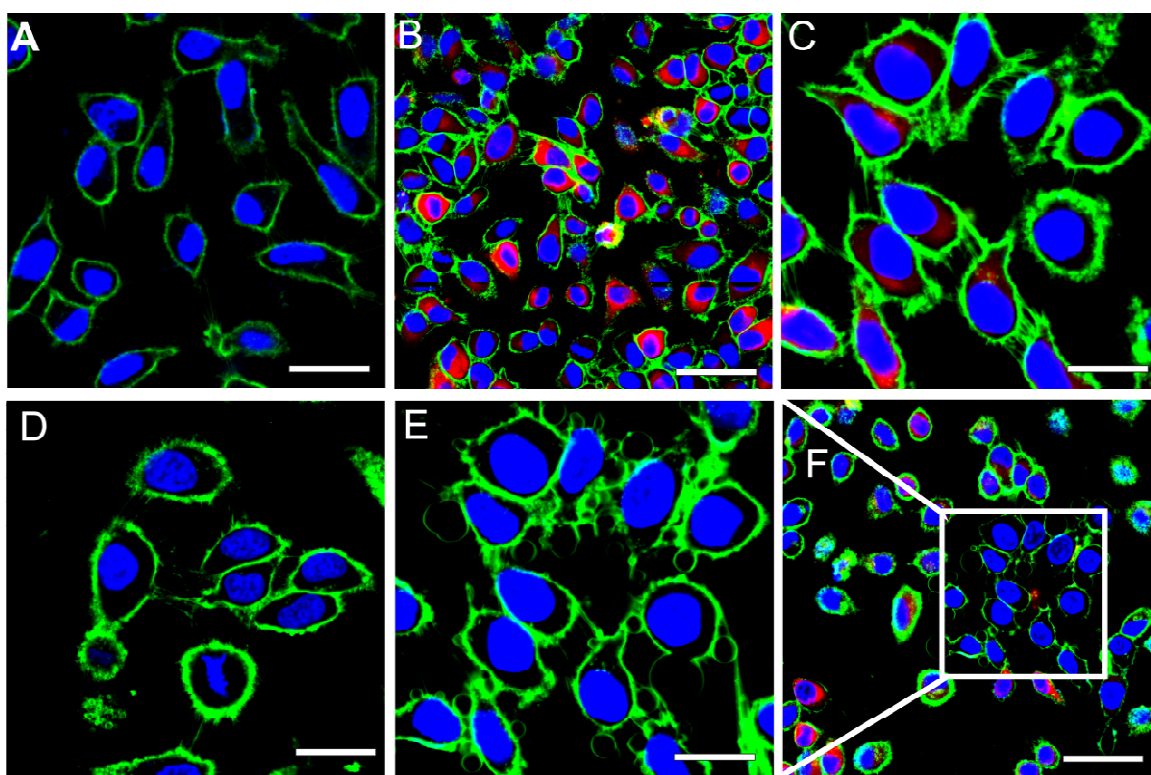


**Fig. 6** Confocal laser scanning micrographs of HeLa cells, where the membrane (green, stained with Cell Mask Deep Red 5 µg/ml for 5 min) and the DNA (violet, stained with Hoechst 33342 10 µg/ml for 10 min) are fluorescently labeled: A) untreated cells growth, B) cells treated with RB-BSA nanoreactors, and irradiated with laser light at 405 nm, 543 nm, and 633 nm, for 0.5 min, C) zoom-in of HeLa cells treated with RB-BSA nanoreactors, D) cells treated with RB-BSA nanoreactors, and irradiated with laser light at 405 nm and 633 nm laser, for 5 min, E) HeLa cells from C) additionally irradiated with laser light at 543 nm, and measured without 543 nm channel F) surrounding area of C) and E) where no laser light was applied outside the white square (length of scale bar: A: 30 µm, B and F: 50 µm, C, D and E: 20 µm). RB-BSA nanoreactors are fluorescent (red dots) upon irradiation with laser light at 543 nm

## Conclusions

We have designed stimulus-responsive nanoreactors containing RB-BSA conjugates as an efficient source of ROS “on demand”. Nanoreactors are permeable to ROS, while they do not allow the photosensitizer to escape from their cavities. The confinement of RB-BSA inside the aqueous cavity of a nanovesicle fulfils various goals: i. protect the active compound from degradation or undesired interactions/reactions; ii. increase the amount of active compound inside cells by up-take of nanoreactors; and iii. decrease side effects that might be associated with inherent RB toxicity.

Stimulus-responsiveness is generated by light-irradiation: our RB-BSA nanoreactors produce ROS only when irradiated with an appropriate wavelength. Our nanoreactors behave like a Trojan horse: they start to generate *in situ* ROS only during appropriate irradiation. The short response time until cells are affected by ROS generated inside the cavities of polymer vesicles indicates their high efficiency. This will serve to decrease the overall dose of irradiation that is necessary to produce a required cytotoxic effect. Nanoreactor functioning can be switched on/off by the presence of a stimulus, and controlled by the illumination conditions, which allows further optimisation in terms of controlled production of ROS. The nanoreactors containing RB-BSA conjugates support theranostic approaches because they

simultaneously allow detection associated with the fluorescent signal of the photosensitizer, and treatment by generation of ROS.

### Acknowledgements

This work was supported by the Swiss National Science Foundation, NCCR Nanosciences, Nano-Tera NTF project “Core-shell superparamagnetic and up-converting nano-engineered materials for biomedical applications – NanoUp” and this is gratefully acknowledged. We thank Dr. S. Egli for synthesis of PMOXA<sub>10</sub>-PDMS<sub>87</sub>-PMOXA<sub>10</sub> copolymer, and M. Inglin for reading the manuscript.

### Notes

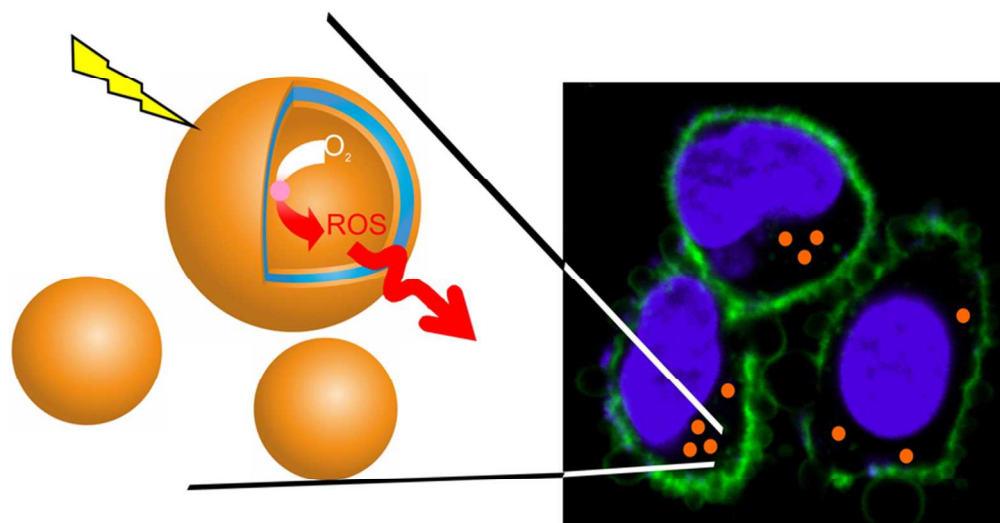
<sup>a</sup> Department of chemistry, University of Basel, Klingelbergstrasse 80, CH-4056 Basel, Switzerland. Fax: +41(0)61 267 3850; Tel: +41 (0)61 267 3839; E-mail: Cornelia.Palivan@unibas.ch

<sup>b</sup> Institute of Physics of Complex Matter, Faculty of Basic Sciences, École Polytechnique Fédérale de Lausanne, CH-1015 Lausanne, Switzerland.

† Electronic Supplementary Information (ESI) available. See DOI: 10.1039/b000000x/

### References

- V. Voliani, G. Signore, R. Nifosi, F. Ricci, S. Luin and F. Beltram, *Recent Patents on Nanomedicine*, 2012, **2**, 34-44.
- C. de las Heras Alarcon, S. Pennadam and C. Alexander, *Chemical Society Reviews*, 2005, **34**, 276-285.
- J. Du and R. K. O'Reilly, *Soft Matter*, 2009, **5**, 3544-3561.
- D. Roy, J. N. Cambre and B. S. Sumerlin, *Progress in Polymer Science*, 2010, **35**, 278-301.
- E. Cabane, X. Zhang, K. Langowska, C. G. Palivan and W. Meier, *Biointerphases*, 2012, **7**, 9-9.
- P. Broz, S. Driamov, J. Ziegler, N. Ben-Haim, S. Marsch, W. Meier and P. Hunziker, *Nano Letters*, 2006, **6**, 2349-2353.
- C. G. Palivan, O. Fischer-Onaca, M. Delcea, F. Itel and W. Meier, *Chemical Society Reviews*, 2012, **41**, 2800-2823.
- C. Nardin, T. Hirt, J. Leukel and W. Meier, *Langmuir*, 2000, **16**, 1035-1041.
- D. M. Vriezema, M. C. Aragonas, J. Elemans, J. Cornelissen, A. E. Rowan and R. J. M. Nolte, *Chemical Reviews*, 2005, **105**, 1445-1489.
- K. T. Kim, S. A. Meeuwissen, R. J. M. Nolte and J. C. M. van Hest, *Nanoscale*, 2010, **2**, 844-858.
- F. Axthelm, O. Casse, W. H. Koppenol, T. Nauser, W. Meier and C. G. Palivan, *Journal of Physical Chemistry B*, 2008, **112**, 8211-8217.
- M. Kumar, M. Grzelakowski, J. Zilles, M. Clark and W. Meier, *Proceedings of the National Academy of Sciences of the United States of America*, 2007, **104**, 20719-20724.
- P. Tanner, O. Onaca, V. Balasubramanian, W. Meier and C. G. Palivan, *Chemistry-a European Journal*, 2011, **17**, 4552-4560.
- S. Egli, M. G. Nussbaumer, V. Balasubramanian, M. Chami, N. Bruns, C. Palivan and W. Meier, *Journal of the American Chemical Society*, 2011, **133**, 4476-4483.
- P. Broz, S. M. Benito, C. Saw, P. Burger, H. Heider, M. Pfisterer, S. Marsch, W. Meier and P. Hunziker, *Journal of Controlled Release*, 2005, **102**, 475-488.
- M. C. DeRosa and R. J. Crutchley, *Coordination Chemistry Reviews*, 2002, **233**, 351-371.
- T. Yogo, Y. Urano, M. Kamiya, K. Sano and T. Nagano, *Bioorganic & Medicinal Chemistry Letters*, 2010, **20**, 4320-4323.
- T. N. Demidova and M. R. Hamblin, *Antimicrobial Agents and Chemotherapy*, 2005, **49**, 2329-2335.
- W. M. Sharman, J. E. van Lier and C. M. Allen, *Advanced Drug Delivery Reviews*, 2004, **56**, 53-76.
- R. F. Donnelly, P. A. McCarron and D. Woolfson, *Recent patents on drug delivery & formulation*, 2009, **3**, 1-7.
- X. Wang, T. Xia, S. A. Ntim, Z. Ji, S. George, H. Meng, H. Zhang, V. Castranova, S. Mitra and A. E. Nel, *Acs Nano*, 2010, **4**, 7241-7252.
- K. Y. Choi, G. Liu, S. Lee and X. Chen, *Nanoscale*, 2012, **4**, 330-342.
- D. Bechet, P. Couleaud, C. Frochot, M.-L. Viriot, F. Guillemain and M. Barberi-Heyob, *Trends in Biotechnology*, 2008, **26**, 612-621.
- L. Xiao, L. Gu, S. B. Howell and M. J. Sailor, *Acs Nano*, 2011, **5**, 3651-3659.
- S. Egli, B. Fischer, S. Hartmann, P. Hunziker, W. Meier and P. Rigler, in *Modern Trends in Polymer Science-Epf 09*, 2010, pp. 278-285.
- G. Battaglia and A. J. Ryan, *Journal of Physical Chemistry B*, 2006, **110**, 10272-10279.
- S. C. G. Tseng, R. P. G. Feenstra and B. D. Watson, *Investigative Ophthalmology & Visual Science*, 1994, **35**, 3295-3307.
- E. Abuin, A. Aspée and L. Leon, *Journal of the Chilean Chemical Society*, 2007, **52**.
- O. Stauch, R. Schubert, G. Savin and W. Burchard, *Biomacromolecules*, 2002, **3**, 565-578.
- S. Litvinchuk, Z. Lu, P. Rigler, T. D. Hirt and W. Meier, *Pharmaceutical Research*, 2009, **26**, 1711-1717.
- A. C. Borges Pereira Costa, V. M. Campos Rasteiro, C. A. Pereira, R. D. Rossoni, J. C. Junqueira and A. O. Cardoso Jorge, *Mycoses*, 2011, **55**, 56-63.
- J. M. Tsay, M. Trzoss, L. Shi, X. Kong, M. Selke, M. E. Jung and S. Weiss, *Journal of the American Chemical Society*, 2007, **129**, 6865-6871.
- A. Sienkiewicz, B. Vilenko, K. Pierzchala, M. Czuba, P. Marcoux, A. Graczyk, G. F. L. Piotr and L. Forro, *Journal of Physics-Condensed Matter*, 2007, **19**.
- C. Nardin, J. Widmer, M. Winterhalter and W. Meier, *European Physical Journal E*, 2001, **4**, 403-410.
- V. Balasubramanian, O. Onaca, M. Ezhevskaya, S. Van Doorslaer, B. Sivasankaran and C. G. Palivan, *Soft Matter*, 2011, **7**, 5595-5603.
- C. De Vocht, A. Ranquin, R. Willaert, J. A. Van Ginderachter, T. Vanhaecke, V. Rogiers, W. Versees, P. Van Gelder and J. Steyaert, *Journal of Controlled Release*, 2009, **137**, 246-254.
- E. Panzarini, B. Tenuzzo and L. Dini, in *Natural Compounds and Their Role in Apoptotic Cell Signaling Pathways*, 2009, pp. 617-626.
- C. Horfelt, B. Stenquist, O. Larko, J. Faergemann and A.-M. Wennberg, *Acta Dermato-Venerologica*, 2007, **87**, 325-329.
- B. Tian, C. Wang, S. Zhang, L. Feng and Z. Liu, *Acs Nano*, 2011, **5**, 7000-7009.
- T. M. Busch, S. M. Hahn, S. M. Evans and C. J. Koch, *Cancer Research*, 2000, **60**, 2636-2642.



We have designed stimulus-responsive nanoreactors based on RB-BSA conjugates that can simultaneously be fluorescently detected and produce ROS "on demand" for theranostic applications.  
75x45mm (300 x 300 DPI)